JOURNAL OF BACTERIOLOGY, Mar. 1980, p. 1399-1408
0021-9193/80/03-1399/10$02.00/0

Vol. 141, No. 3

Ultrastructure of a Magnetotactic Spirillum

D. L. BALKWILL,* D. MARATEA, AND R. P. BLAKEMORE

Department of Microbiology, University of New Hampshire, Durham, New Hampshire 03824

The ultrastructure of a magnetotactic bacterium (strain MS-1) was examined by transmission, scanning, and scanning-transmission electron microscopy. The organism resembled other spirilla in general cell morphology, although some differences were detected at the ultrastructural level. Electron-dense particles within magnetotactic cells were shown by energy-dispersive X-ray analysis to be localizations containing iron. A non-magnetotactic variant of strain MS-1 lacked these novel bacterial inclusion bodies. A chain of these particles traversed each magnetotactic cell in a specific arrangement that was consistent from cell to cell, seemingly associated with the inner surface of the cytoplasmic membrane. Each particle was surrounded by an electron-dense layer separated from the particle surface by an electron-transparent region. The term "magnetosome" is proposed for the electron-dense particles with their enveloping layer(s) as found in this and other magnetotactic bacteria.

Magnetotactic bacteria of diverse morphological types live in marine and freshwater sediments, from which they can be separated by using small permanent magnets (4). All magnetically responsive cells examined to date (4, 10, 23) have contained one or two intracellular chains of electron-dense, iron-rich particles, each measuring 40 to 100 nm in width. Recently, a helical, heterotrophic, freshwater, magnetotactic bacterium was isolated and designated strain MS-1 (10). This isolate has been characterized and appears to be a new species of the genus *Aquaspirillum* (17) by criteria separate from its magnetic properties (5; unpublished data). Strain MS-1 possesses a single chain of electron-dense particles, each approximately 40 nm wide. Results of ^{57}Fe Mössbauer resonance spectroscopy established that iron in magnetotactic cells of strain MS-1 is present primarily as magnetite (10). A non-magnetotactic variant of this organism (obtained by culturing in a medium with reduced iron content) lacked electron-dense particles and magnetite.

Ultrastructural characteristics of magnetotactic bacteria have not been described in detail. The objective of this study was to characterize the ultrastructure of magnetotactic and non-magnetotactic variants of strain MS-1. The detailed structure of the electron-dense, iron-rich particles and their relationship to the remainder of the cell were of central interest because (i) they appear to differ from other types of inclusion bodies reported to occur in bacterial cells (31), and (ii) they are assumed to be responsible for magnetic orientation of this organism.

MATERIALS AND METHODS

Medium and growth. Magnetotactic and non-magnetotactic variants of strain MS-1 were cultured in growth medium containing: 0.25 ml of 0.01 M ferric quinate, 1.0 ml of vitamin elixir (38), 1.0 ml of mineral elixir (38), 0.5 ml of 1.0 M KH_2PO_4, 0.2 ml of 0.01% (wt/vol) resazurin, 0.075 g of tartaric acid, 0.01 g of $NaNO_3$, 0.005 g of sodium thioglycolate, and water to make 100 ml. The pH was adjusted to 6.75 with 10 N NaOH before sterilization.

Cells were cultured in serum-stoppered bottles under microaerobic conditions. The atmosphere of each bottle was displaced with N_2. After autoclaving, sterile air was injected to produce a final O_2 concentration of 1 to 3% (vol/vol). Incubation was at 30°C after the addition of a 5% (vol/vol) inoculum.

Preparation of whole cells for electron microscopy. Cells were concentrated from the growth medium by centrifugation. For negative staining, concentrated cell suspensions were placed on parlodion-coated, carbon-reinforced, 400-mesh copper grids and mixed with 0.5% (wt/vol) uranyl acetate (pH 4.2). The excess liquid was drawn off the grid surface, after which the cell preparations were allowed to air dry. For critical-point drying, cell suspensions were placed on grids (as above) for 20 min to absorb cells onto the grid surface. These grids were then prefixed for 30 min in 3.6% (vol/vol) glutaraldehyde (in 0.1 M sodium cacodylate, pH 7.0), rinsed twice in 0.1 M sodium cacodylate, postfixed for 20 min in 1% (wt/vol) OsO_4 (in 0.1 M sodium cacodylate), and rinsed again. After dehydration through a graded ethanol series, the samples were critical-point dried with CO_2 in a Sam-Dri PVT-3 critical-point dryer (Tousimis Research Corp., Rockville, Md.). Dried-cell preparations were shadowed with platinum-carbon at an evaporation angle of 45°.

Preparation of electron-dense particles for

electron microscopy. Intracellular, electron-dense particles of the magnetotactic variant of strain MS-1 were released from cells by sonicating a cell suspension for 1.5 min (three 30-s bursts) at 175-W acoustical energy (20 KHz). The sonicated preparations were treated for 30 min at 60°C in 0.5% (wt/vol) sodium dodecyl sulfate. Suspensions of the sodium dodecyl sulfate-treated particles were placed on grids (as above) and were allowed to air dry after the excess liquid was drawn off the grid surface.

Preparation of thin sections. Cells of strain MS-1 were prepared for thin sectioning by (i) the Kellenberger procedure, (ii) the ruthenium red procedure, or (iii) the glutaraldehyde-osmium tetroxide double-fixation procedure. In the Kellenberger procedure, cells were prefixed by adding 1% OsO_4 (in Kellenberger buffer; 19) to the culture medium to bring the final OsO_4 concentration to 0.1%. Cells were then concentrated by centrifugation, washed in Kellenberger buffer, suspended in tryptone-salt solution (1% tryptone, 0.5% NaCl), and embedded in 2% (wt/vol) Noble agar (Difco). The agar was cut into small blocks, which were postfixed for 18 h in 1% OsO_4 (in Kellenberger buffer) and prestained for 3 h in 0.5% (wt/vol) uranyl acetate (in Kellenberger buffer). The ruthenium red procedure was a variation of that reported by Cagle et al. (6). Cells were prestained for 1 h in 0.15% (wt/vol) ruthenium red (in 0.1 M sodium cacodylate, pH 7.0) and prefixed for 1 h in a mixture of 3.6% glutaraldehyde and 0.15% ruthenium red (in 0.1 M sodium cacodylate). Prefixed cells were washed twice in 0.1 M sodium cacodylate and postfixed for 1 h in a mixture of 1% OsO_4 and 0.15% ruthenium red (in 0.1 M sodium cacodylate). Postfixed cells were embedded in agar as described above. For the glutaraldehyde-osmium tetroxide double fixation, cells were prefixed for 1 h in 3.6% glutaraldehyde (in 0.1 M sodium cacodylate), rinsed twice in 0.1 M sodium cacodylate, and postfixed for 1 h in 1% OsO_4 (in 0.1 M sodium cacodylate). Postfixed cells were embedded in agar as above.

Samples from all fixations were dehydrated through a graded ethanol series and embedded in Spurr's low-viscosity epoxy resin (33). Sections were cut with glass knives on a LKB Ultratome III ultramicrotome, using a cutting speed of 2 mm/s and a clearance angle of 2 to 3°. Sections were retrieved with uncoated, 400-mesh copper grids, then poststained for 15 min with 5% (wt/vol) uranyl acetate in 50% (vol/vol) methanol and for 2 min with 0.4% (wt/vol) lead citrate (29).

Electron microscopy. Samples for transmission electron microscopy were viewed and recorded with a JEOL JEM-100S electron microscope at an accelerating potential of 80 kV. Scanning electron microscopy, scanning-transmission electron microscopy, and energy-dispersive X-ray analysis were performed at 80 kV on a JEOL JEM-100CX electron microscope fitted with a Kevex X-ray analyzer.

Dimensions of whole cells and flagella were measured from micrographs of critical-point-dried, shadowed cell preparations. At least 50 measurements were taken for each dimension. Subcellular dimensions were measured from micrographs of thin-sectioned Kellenberger preparations. At least 30 measurements were taken for each dimension. Measurements from micrographs of samples prepared by the other two fixation procedures did not differ significantly from these values. Numbers of electron-dense particles in each of 300 cells were determined from negatively stained preparations. Sizes of 200 electron-dense particles that had been released from cells with sonication were measured from transmission electron micrographs.

Micrographs of both critical-point-dried, shadowed and negatively stained whole cells were chosen to illustrate the general morphology of strain MS-1. A thin section of cells fixed by the ruthenium red procedure was chosen to illustrate extracellular polysaccharide material. Thin sections of Kellenberger-fixed cells were chosen to illustrate internal cell ultrastructure because these preparations provided the greatest contrast and resolution. The results of both the ruthenium red and the glutaraldehyde-osmium tetroxide double fixations were otherwise equivalent to those obtained with the Kellenberger technique.

RESULTS

Cell morphology and flagellation. Magnetotactic cells of strain MS-1 possessed a right-handed (34) helical morphology as seen both in critical-point-dried and shadowed preparations and in negatively stained preparations (Fig. 1). Critical-point-dried cells had relatively constant diameters (0.28 to 0.36 μm; average, 0.32 μm), but their lengths varied considerably (2.3 to 11.1 μm; average, 4.3 μm). This variation resulted from the fact that individual cells comprised from one to eight turns of a helix, even though 85% of the cells examined consisted of three turns or less. The wavelength of the helix varied from 0.9 to 2.4 μm (average, 1.7 μm), and the amplitude ranged from 0.14 to 0.44 μm (average, 0.36 μm).

Each cell, regardless of its length, appeared to have single bipolar flagella (Fig. 1). However, it was necessary to handle cells carefully to obtain a reliable indication of their flagellation pattern; flagella were easily sheared off during centrifugation or shaking of cell suspensions. Each flagellum was 22 nm in diameter and 1.5 to 2.5 μm (average, 1.9 μm) long. Pili or other appendages besides flagella were not observed.

Ultrastructure of the cell envelope. The cell envelope of strain MS-1 appeared in thin sections to consist of two distinct layers (Fig. 2 and 5), outer membrane or "wall membrane" (25) and cytoplasmic membrane. The outer membrane was trilaminate in cross sections, consisting of two 1.8-nm-thick electron-dense layers separated by a 2.5-nm-thick electron-transparent layer. The overall configuration of the outer membrane in thin sections was markedly convoluted, as was the cell surface in critical-point-dried, shadowed preparations of whole cells (Fig. 1a). Small loops or blebs of membranous mate-

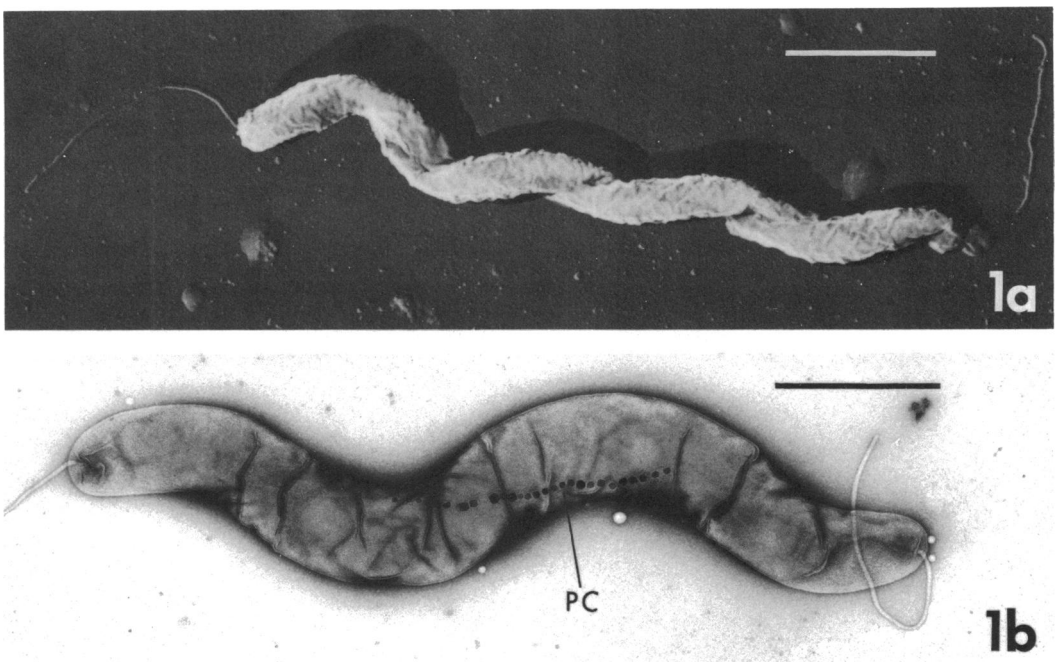

FIG. 1. *Transmission electron micrographs of whole cell preparations of the magnetotactic variant of strain MS-1. Note single bipolar flagellation pattern. Bars = 1.0 μm. (a) Critical-point-dried and platinum-carbon-shadowed cell (negative image). (b) Negatively stained cell, showing electron-dense particle chain (PC).*

rial sometimes extended outward from the surface of the outer membrane (Fig. 2). These structures ranged from 24 to 91 nm in diameter. The ultrastructural characteristics and dimensions of the cytoplasmic membrane were the same as those of the outer membrane, except that the former was slightly less convoluted. The outer and cytoplasmic membranes were separated by an electron-transparent periplasmic region that varied considerably in width. Peptidoglycan material, if present in this region, was not visible as a distinct structure in these preparations.

The cell envelope of strain MS-1 did not appear to include any type of hexagonally packed superficial layer (24) on the external side of the outer membrane. However, the cells did secrete an extracellular polysaccharide substance that was visible after staining with ruthenium red (Fig. 3). This material was amorphously deposited outside of the cells; an organized capsular configuration was not observed.

Intracellular ultrastructure of strain MS-1. The cytoplasm consisted largely of nuclear material and ribosomes (Fig. 2). These usually comprised equal volumes. The nuclear material was generally confined to discrete, centrally located packets. The ribosomes were distributed freely throughout the periphery of the cell. In many cells, portions of the cytoplasm were occupied by loops of membranous material (Fig. 2). These membrane loops appeared to be invaginations of the cytoplasmic membrane, and they ranged from 0.05 to 0.17 μm in diameter (average, 0.1 μm). The membrane-bound areas were readily distinguished from the rest of the cytoplasm because they lacked a definite substructure and were relatively electron transparent.

Two types of inclusion bodies were present within the cytoplasm, (i) those with a structure resembling poly-β-hydroxybutyrate (PHB) granules (8, 31) and (ii) electron-dense particles (described below). The structures presumed to be PHB granules appeared in thin-sectioned cells as electron-transparent areas bounded by a single, electron-dense layer (Fig. 2). Except for this boundary, they were similar in appearance to the membrane-bound regions of the cytoplasm described above. Similar structures were sometimes visible as electron-transparent areas in negatively stained whole cells. These are believed to be the regions of the cytoplasm which were stained by Sudan black B, as evidenced by light microscopy. They ranged from 0.09 to 0.30 μm in diameter, and the numbers per cell varied from none to eight.

Electron-dense particles. Magnetotactic

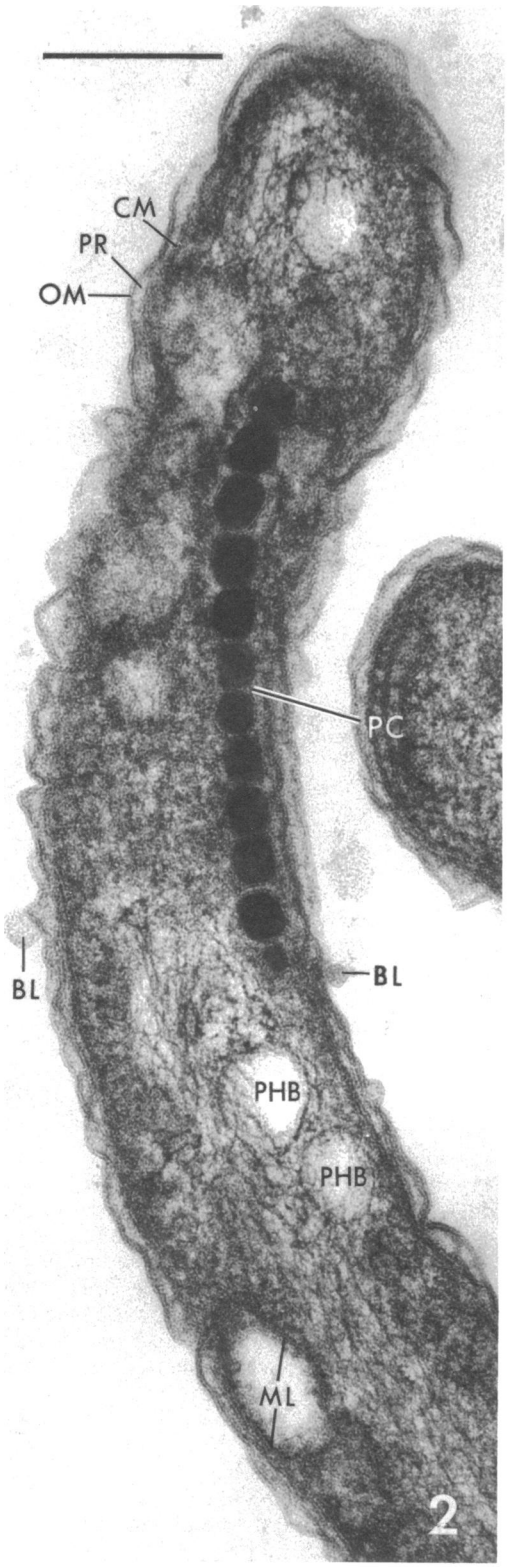

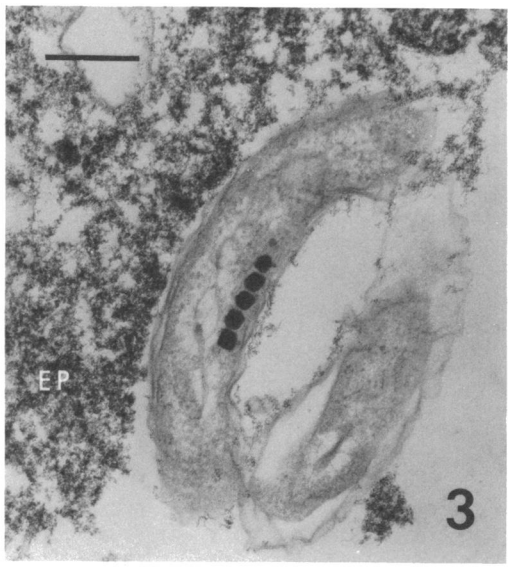

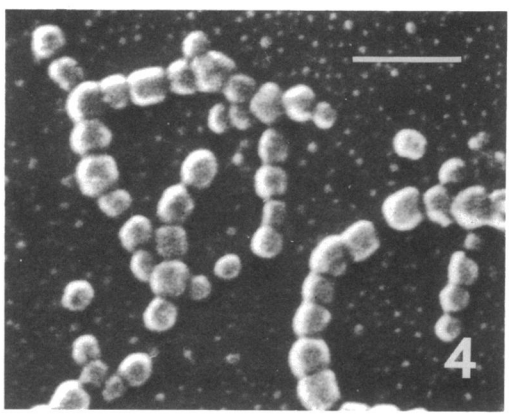

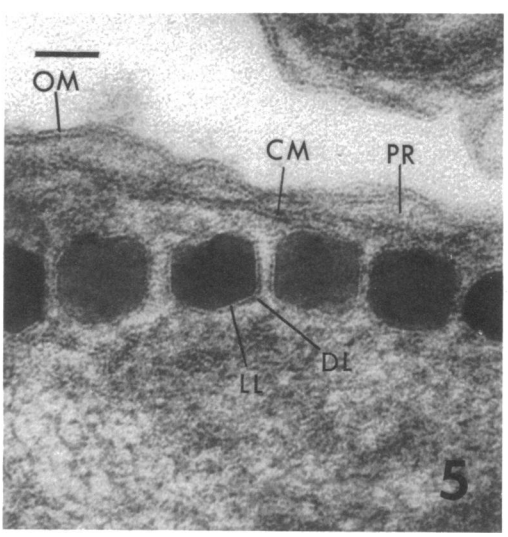

FIGS. 2–5.

cells of strain MS-1 contained a series of electron-dense particles that were readily observed in negatively stained or thin-sectioned (Fig. 1b, 2, and 5) preparations. These particles were released from cells by sonication and purified by treatment with sodium dodecyl sulfate. Scanning electron microscopy of these purified particles (Fig. 4) indicated that most of them were cubic with rounded corners, although some of them were probably octahedral. The particles tended to remain in chains after release from the cells. These chains frequently formed closed loops on the grid surface. The particles varied from 25 to 55 nm (average, 42 nm) in width, but 66% ranged between 39 and 49 nm.

In negatively stained preparations of whole cells (Fig. 1b), the electron-dense particles were arranged in a single chain that longitudinally traversed the cell in a reasonably straight line. The largest particles were situated in the center of the chain, while those at the ends were often smaller. The numbers of particles in each chain varied from 5 to 41 (average, 17.6), but approximately 19% of the cells lacked the particles entirely. The particle chains were intracellular; i.e., they were located inside of the cytoplasmic membrane as evidenced by thin-sectioned preparations (Fig. 2 and 5). The particles were usually seen in close proximity to the inner surface of the cytoplasmic membrane in longitudinal sections, provided that these sections traversed the actual diameter of the cell at the point where the particles were visible. In approximately 50 cross sections examined, the particles were always situated adjacent to the inner surface of the membrane.

The intracellular particle chains possessed a regular substructure in thin-sectioned preparations (Fig. 5). Each particle was surrounded by a 1.4-nm-thick electron-dense layer which was always separated from the particle surface by an electron-transparent layer of uniform width (1.6 nm). The electron-dense layers of adjacent particles in a chain were sometimes in direct contact with each other, but were usually separated by a distance of 3 to 18 nm. The regions between separated particles appeared to contain cytoplasmic materials. No distinct structures appeared to physically link the particles. Similarly, no linking structures were seen in negatively stained preparations of whole cells. In these preparations, however, the particles always appeared to be separated from each other. The substructures of the particle chains observed in thin sections were not detected in the whole cell preparations.

Scanning-transmission electron microscopy (Fig. 6a) and energy-dispersive X-ray analysis (Figs. 6b and 6c) of thin-sectioned preparations indicated that the electron-dense particles of strain MS-1 were localizations containing iron. Other elements detected included osmium, lead, uranium, and copper. These were attributable to either the fixation and staining procedures or the copper specimen grid. No iron was detected in particle-free regions of the cytoplasm, although the other elements listed above were present (Fig. 6c).

Coccoid bodies. Substantial numbers of magnetically responsive coccoid bodies (17) formed in magnetotactic cultures of strain MS-1 when they were stored for several weeks at 4°C, or when they were incubated at 36°C. Thin-sectioned preparations of coccoid bodies (Fig. 7) indicated that their cell morphology, although roughly spherical, was actually quite irregular. They were bounded by an intact layer of outer membrane, but this material lacked the rigid configuration of the outer membrane in normal cells. This layer was also considerably less convoluted than that of helical cells. The cytoplasm of coccoid bodies was contained within a typical cytoplasmic membrane, which was separated from the outer membrane by a large and variable electron-transparent periplasmic region. The cytoplasm was composed largely of nuclear material and ribosomes, and portions of it were closed within loops of membranous material. The areas within the membrane loops were electron transparent (as in helical cells), but it could not be determined whether they originated as invaginations of the cytoplasmic membrane. Electron-

FIG. 2. *Transmission electron micrograph of thin-sectioned magnetotactic cell. BL, Membranous blebs extending from cell surface; CM, cytoplasmic membrane; ML, membranous loop; OM, outer membrane; PC, electron-dense particle chain; PHB, structures resembling PHB granules; PR, periplasmic region. Kellenberger fixation. Bar = 0.25 μm.*

FIG. 3. *Transmission electron micrograph of thin-sectioned magnetotactic cell with extracellular polysaccharide material (EP) stained with ruthenium red. Bar = 0.25 μm.*

FIG. 4. *Scanning electron micrograph of electron-dense particles released from the magnetotactic variant of strain MS-1. Bar = 0.15 μm.*

FIG. 5. *Transmission electron micrograph of the electron-dense particle chain in a thin-sectioned magnetotactic cell. CM, Cytoplasmic membrane; DL, electron-dense layer surrounding each particle; LL, electron-transparent layer separating DL from particle surface; OM, outer membrane; PR, periplasmic region. Kellenberger fixation. Bar = 50 nm.*

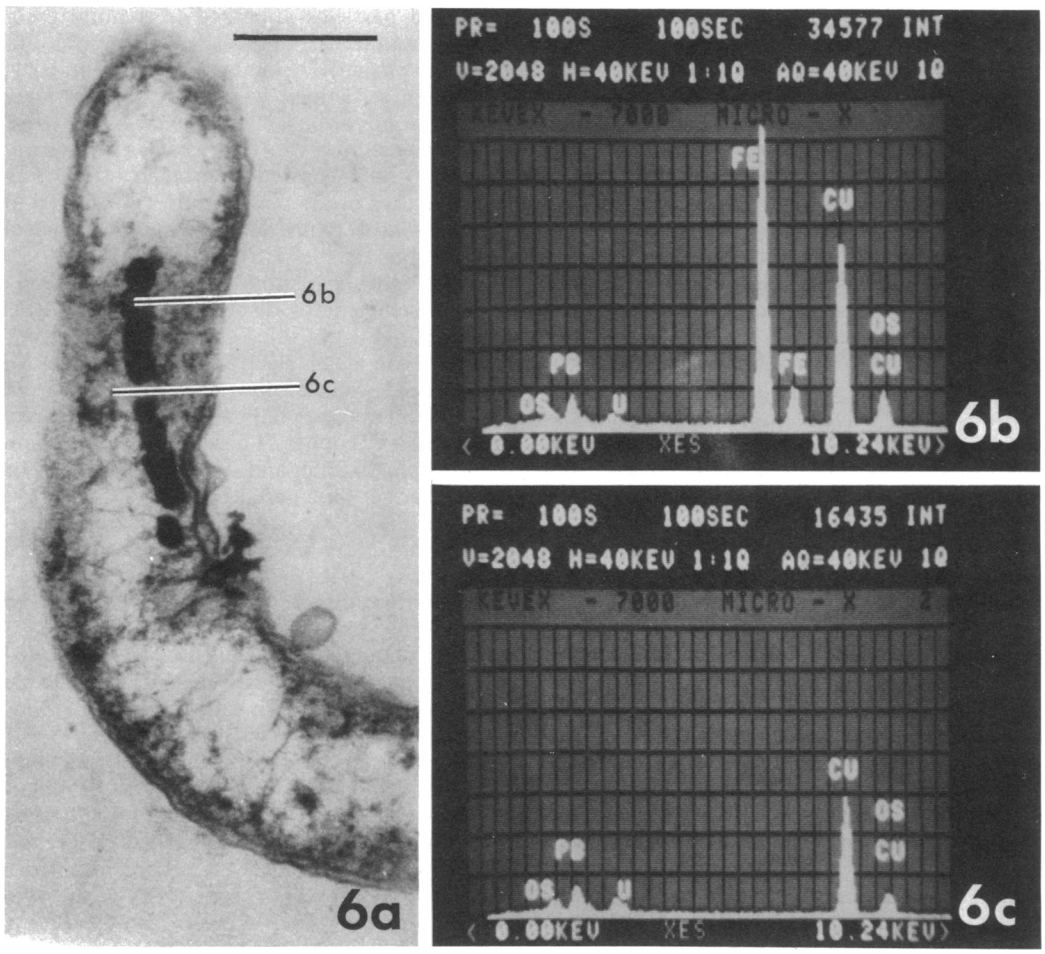

FIG. 6. *Scanning-transmission electron micrograph and energy-dispersive X-ray spectra of thin-sectioned magnetotactic cell. (a) Scanning-transmission electron micrograph showing points where cell was analyzed to obtain spectra in b and c. Kellenberger fixation. Bar = 0.25 μm (b) Spectrum obtained from one electron-dense particle in the chain. (c) Spectrum obtained from particle-free region of the cytoplasm near the particle chain.*

dense particles, which were present in the cytoplasm of most coccoid bodies, remained in chains. Structures resembling PHB granules were not observed in coccoid bodies.

Non-magnetotactic variant of strain MS-1. Non-magnetotactic cells appeared similar or identical to magnetotactic cells with respect to (i) general cell morphology, (ii) cell dimensions, (iii) flagellation, and (iv) lack of pili or other appendages besides flagella (Fig. 8). They differed from magnetotactic cells in that they lacked chains of electron-dense particles. A thin, electron-dense filament was visible in negatively stained preparations of non-magnetotactic cells that were examined before this variant had been repeatedly transferred in culture medium. This filament traversed the cell (Fig. 9) in the same manner as did the particle chain in magnetotactic cells. After repeated transfers of the non-magnetotactic variant, however, the filament was no longer observed in negatively stained or thin-sectioned preparations.

Thin sections of non-magnetotactic cells (Fig. 10) showed that their ultrastructure was also similar to that of magnetotactic cells, except for the absence of electron-dense particle chains. The cytoplasm was composed largely of nuclear material and ribosomes, but also contained the presumed PHB granules and regions bound by membranous loops.

DISCUSSION

The general cell morphology of strain MS-1 is similar to that of other heterotrophic spirilla

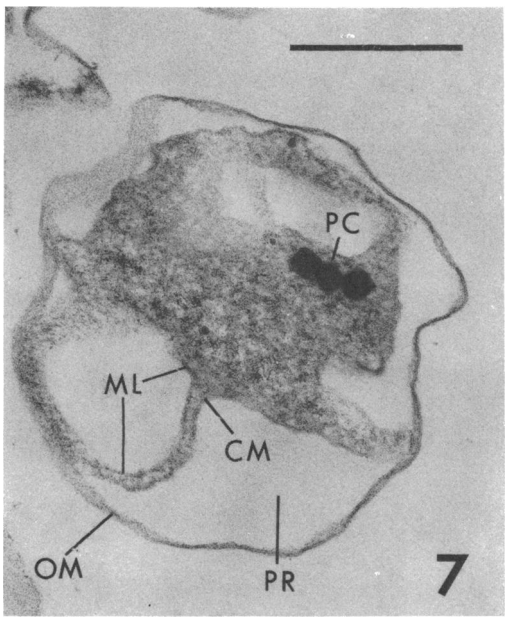

FIG. 7. *Transmission electron micrograph of thin-sectioned coccoid body of the magnetotactic variant of strain MS-1. CM, cytoplasmic membrane; ML, membranous structure possibly corresponding to membrane loops in helical cells; OM, outer membrane; PC, electron-dense particle chain; PR, periplasmic region. Kellenberger fixation. Bar = 0.3 μm.*

(20). Principal morphological similarities between this organism and other spirilla include (i) helical cell shape, (ii) cell size, (iii) flagellation, (iv) presence of structures resembling PHB granules, and (v) a tendency to form "coccoid bodies" (17, 37) in old cultures. The dimensions (i.e., wavelength and amplitude) of the cell helix vary over a considerable range. This variation, which could be a natural cultural characteristic or could result from methods used to prepare cells for electron microscopy, suggests that cells of strain MS-1 are somewhat flexible. Spirilla have traditionally been described as rigid organisms (9, 20), but recent work (18) has demonstrated that they are actually more flexible than other bacteria tested. The flagella, which are relatively short and comprise less than one complete wavelength, are similar to those of other spirilla (21). The single bipolar flagellation pattern of strain MS-1 is somewhat unusual because most spirilla possess bipolar tufts of flagella (20). However, single bipolar flagellation has been reported in *Aquaspirillum* (formerly *Spirillum*) *polymorphum* (17) and *Aquaspirillum* (formerly *Spirillum*) *psychrophilum* (35). The tendency to form coccoid bodies is also somewhat rare among freshwater spirilla, but has been reported in at least four species (20). As with other spirilla, coccoid bodies of strain MS-1 were formed in old cultures after active cell division had ceased. They also formed in younger cultures grown at elevated temperatures.

Some ultrastructural differences between strain MS-1 and other spirilla that have been studied in detail were apparent. Polar membranes, which have been observed in several other spirilla (12, 13, 25, 28, 30), were not found. The organism's cell envelope was typical of gram-negative bacteria in general (7), but the distinct peptidoglycan layer observed in *Aquaspirillum* (formerly *Spirillum*) *serpens* (24–26) was not seen. This may indicate that the peptidoglycan layer of strain MS-1 is thinner than that of other spirilla. The cell envelope of strain MS-1 also lacked the hexagonally packed superficial ("RS") layer reported for *A. serpens* (24) and other spirilla (1–3, 16). Such RS layers are found in a wide range of bacterial species (11, 14, 32, 36), but are not a universal characteristic of the chemoheterotrophic spirilla. Martin et al. (22) have suggested that the RS layer may confer additional rigidity to the cell envelope of spirilla. The absence of this layer in cells of strain MS-1, along with the relative thinness of their peptidoglycan, may account for the apparent cell flexibility observed in this study.

Magnetotactic and non-magnetotactic cells of strain MS-1 possessed a number of intracellular membranous loops that originated at the cytoplasmic membrane and extended into the cytoplasm. Intracellular membranes were also present in coccoid bodies of strain MS-1, but it was not clear whether they were equivalent to the membrane loops of helical cells. All magnetotactic bacteria examined to date (4, 23) possess similar intracellular membrane loops, but the function of such loops is not known. Since the areas they surround are structurally distinct from the cytoplasm, they may be a compartmentalized storage system. Similar structures have been observed in *Azotobacter* (27) and photosynthetic bacteria (15), in which they presumably serve to compartmentalize specific cell components. Moench and Konetzka (23) tentatively identified similar structures in a freshwater magnetotactic coccus as PHB granules. However, PHB granules have not been reported to possess a trilaminate membrane boundary in other bacteria (8, 31). Blakemore (4) observed trilaminate membrane loops surrounding intracellular iron-rich particles and speculated that they were sites of particle synthesis. As indicated below, we have not obtained definitive evidence that trilaminate membranes surround the electron-dense particles in cells of strain MS-1.

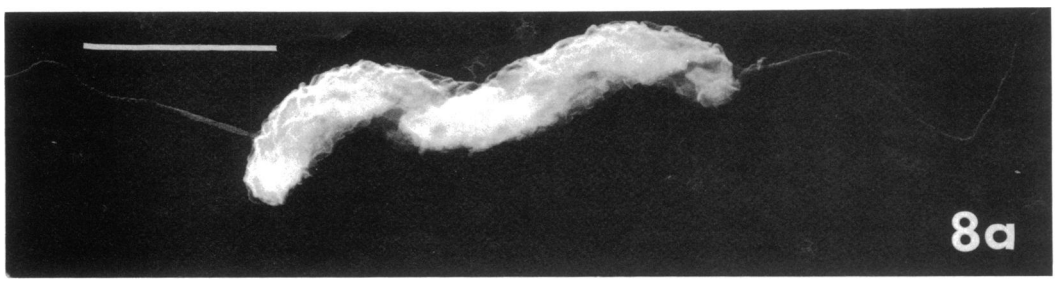

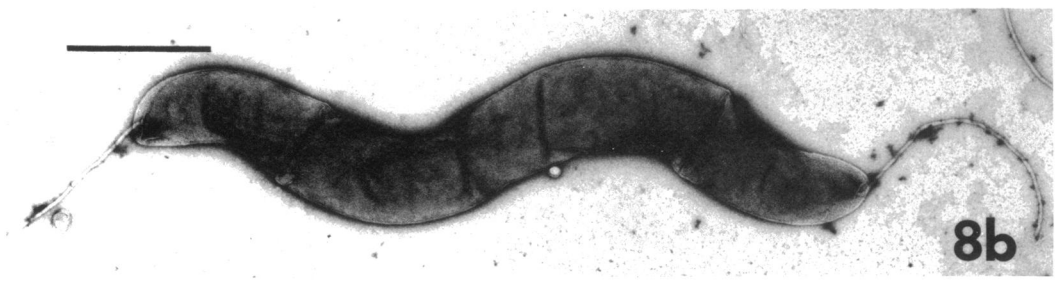

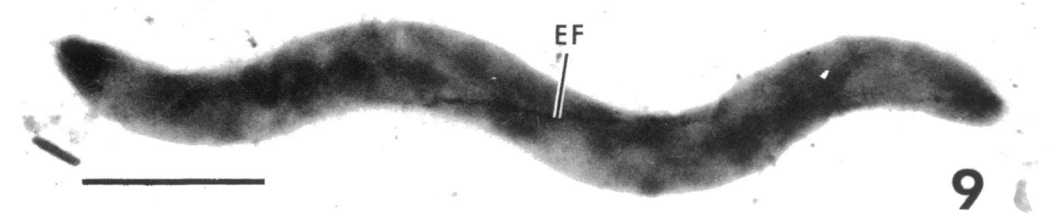

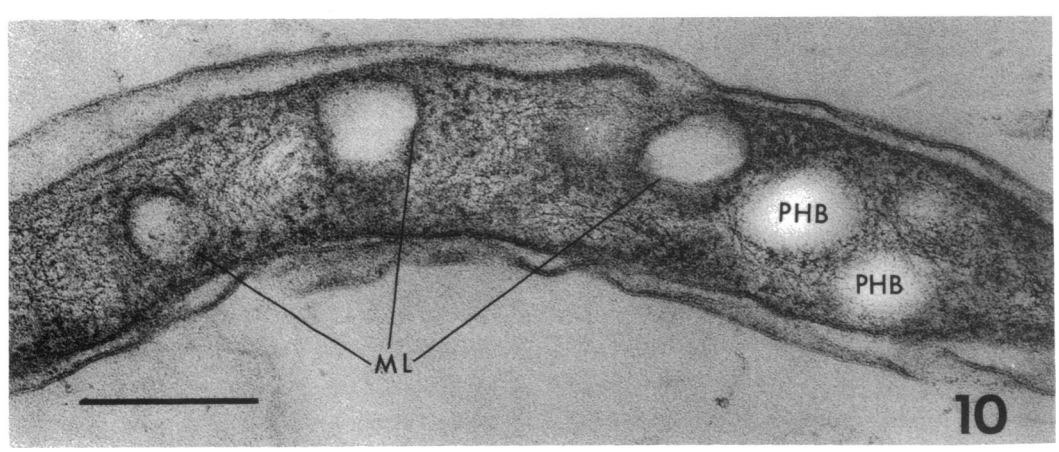

FIG. 8. *Transmission electron micrographs of whole cell preparations of the non-magnetotactic variant of strain MS-1. Note single bipolar flagellation pattern. Bars = 1.0 μm. (a) Critical-point-dried and platinum-carbon-shadowed cell (negative image). (b) Negatively stained cell.*

FIG. 9. *Transmission electron micrograph of negatively stained non-magnetotactic cell examined before the non-magnetotactic variant had been transferred repeatedly in laboratory culture. Lightly stained to delineate the electron-dense filament (EF) present. Bar = 1.0 μm.*

FIG. 10. *Transmission electron micrograph of thin-sectioned non-magnetotactic cell. ML, Membranous loops; PHB, structures resembling PHB granules. Kellenberger fixation. Bar = 0.25 μm.*

Electron microscopy confirmed that magnetotactic cells and coccoid bodies of strain MS-1 each contained an intracellular chain of electron-dense, iron-rich particles similar to those observed previously in other magnetotactic bacteria (4, 23). These particle chains, which are not known to occur in other spirilla, do not resemble any of the various known types of inclusion bodies in non-magnetotactic bacterial cells (31). To the best of our knowledge, they are novel bacterial components, the ultrastructure of which has not yet been thoroughly described. The electron-dense particles examined in this study possessed a distinct and consistent substructure. When observed in thin sections, each particle was surrounded by an electron-dense layer that was separated from the particle itself by an electron-transparent region. The dense layer was not an electron-imaging artifact caused by the metallic nature of the particles because it could not be resolved in negatively stained preparations. The electron-dense layer could be a protein "membrane," similar to those that surround certain other types of bacterial inclusion bodies (31). However, the protein membrane of other inclusion bodies is not separated from their surface by an electron-transparent region. It is conceivable that a true biological membrane (i.e., lipid bilayer) surrounds the particles instead of a protein layer, but definitive evidence for this is lacking at this time.

The electron-dense particles of strain MS-1 were always arranged in chains; random arrangements were not observed in this study. These chains appear to be a stable structural characteristic of the particles. The particles remained in chains when coccoid bodies were formed, even though considerable cell deformation had taken place. It is of special interest that they remained in chains after being released from the cells by sonication. Whereas particle-to-particle magnetic forces promote a chained configuration of single-domain particles (R. B. Frankel and R. P. Blakemore, submitted for publication), it seems likely that they are also connected structurally. As described above, protein or lipid membranes could serve to do this. In this regard, the filaments seen in non-magnetotactic cells before repeated transfer in laboratory culture may have constituted a linking structure enclosing noncrystalline accumulations of iron.

The particle chains in cells of strain MS-1 appeared in this study to have a consistent intracellular location or distribution. In negatively stained preparations, they always appeared to traverse the cell in a reasonably straight line. This was also frequently true of cells viewed in thin sections. In cross sections, however, the particles were always located near the inner surface of the cytoplasmic membrane. This was also observed in longitudinal sections that transected the entire cell diameter in a region occupied by the particles. This suggests that the particle chains are always in close proximity to the inner surface of the cytoplasmic membrane. A similar arrangement may occur in coccoid magnetotactic bacteria, as described earlier (4, 23). It is possible that the particle chains in cells of strain MS-1 are actually attached to the inner surface of the membrane, although no connections were observed in thin sections. Isolated chains frequently formed closed loops, but this pattern was never observed in cells. Therefore, some cell structural element(s) most likely maintains the elongated shape of the chains within cells. Attachment to the cytoplasmic membrane probably does not account for the integrity of the chains, however, because they remained intact after being released from the cells by sonication. It is also somewhat difficult to envision how the entire particle chain could remain close to the (helical) cell surface and still traverse the cell in a straight line. If this actually occurs in cells of strain MS-1, the particles must have a very precise placement in the cell for such a pattern to be observed consistently. Serial sectioning or other techniques of three-dimensional analysis will be required to fully elucidate details of the particle chain location.

Strain MS-1 has previously been shown to contain a relatively large amount (2% of its dry weight) of iron, present primarily as magnetite (10). In the present study, scanning-transmission electron microscopy and energy-dispersive X-ray analysis showed that cellular iron is localized in electron-dense particle chains. Moreover, chains of isolated particles have magnetic remanence, orient in externally applied magnetic fields (unpublished data), and recently were shown to have an X-ray diffraction pattern characteristic of magnetite (E. J. Alexander, Francis Bitter National Magnet Laboratory, Massachusetts Institute of Technology, personal communication). Since they (or structures similar to them) have been reported in all magnetotactic bacteria reported to date (4, 23), but have not been observed in any non-magnetotactic cells, there can be little doubt that they are directly responsible for the passive alignment of magnetotactic cells in magnetic fields. As bacterial inclusion bodies, then, the particles are as unique functionally as they are structurally. We propose that the electron-dense particles and their associated bounding layers in magnetotactic bacteria be termed "magnetosomes" in view of their

structural and chemical nature, as well as their functional role in bacterial magnetotaxis.

ACKNOWLEDGMENTS

We thank JEOL U.S.A. Inc. (Peabody, Mass.) for use of the JEOL JEM-100CX electron microscope and related analytical instruments. We thank T. Yoshioka of the JEOL Applications Laboratory for technical assistance with scanning electron microscopy, scanning-transmission electron microscopy, and energy-dispersive X-ray analysis. We thank R. B. Frankel for valuable discussion.

This work was supported by grant PCM 77-12175 from the National Science Foundation and by the Central University Research Fund of the University of New Hampshire.

LITERATURE CITED

1. **Beveridge, T. J., and R. G. E. Murray.** 1974. Superficial macromolecular arrays on the cell wall of *Spirillum putridiconchylium*. J. Bacteriol. **119**:1019–1038.
2. **Beveridge, T. J., and R. G. E. Murray.** 1976. Superficial cell-wall layers on *Spirillum* "Ordal" and their in vitro reassembly. Can. J. Microbiol. **22**:567–582.
3. **Beveridge, T. J., and R. G. E. Murray.** 1976. Dependence of the superficial layers of *Spirillum putridiconchylium* on Ca^{2+} or Sr^{2+}. Can. J. Microbiol. **22**:1235–1244.
4. **Blakemore, R. P.** 1975. Magnetotactic bacteria. Science **190**:377–379.
5. **Blakemore, R. P., D. Maratea, and R. S. Wolfe.** 1979. Isolation and pure culture of a freshwater magnetic spirillum in chemically defined medium. J. Bacteriol. **140**:720–729.
6. **Cagle, G. D., R. M. Pfister, and G. R. Vela.** 1972. Improved staining of extracellular polymer for electron microscopy: examination of *Azotobacter*, *Zoogloea*, *Leuconostoc*, and *Bacillus*. Appl. Microbiol. **24**:477–487.
7. **Costerton, J. W., J. M. Ingram, and K.-J. Cheng.** 1974. Structure and function of the cell envelope of gram-negative bacteria. Bacteriol. Rev. **38**:87–110.
8. **Dunlop, W. F., and A. W. Robards.** 1973. Ultrastructural study of poly-β-hydroxybutyrate granules from *Bacillus cereus*. J. Bacteriol. **114**:1271–1280.
9. **Ehrenberg, C. G.** 1838. Die Infusionthierchen als vollkommene Organismen, p. i-xvii, 1–547. L. Voss, Leipzig.
10. **Frankel, R. B., R. P. Blakemore, and R. S. Wolfe.** 1979. Magnetite in freshwater magnetotactic bacteria. Science **203**:1355–1356.
11. **Glauert, A. M., and M. J. Thornley.** 1969. The topography of the bacterial cell wall. Annu. Rev. Microbiol. **23**:159–198.
12. **Hickman, D. D., and A. W. Frenkel.** 1965. Observations on the structure of *Rhodospirillum molischianum*. J. Cell Biol. **25**:261–278.
13. **Hickman, D. D., and A. W. Frenkel.** 1965. Observations on the structure of *Rhodospirillum rubrum*. J. Cell Biol. **25**:279–291.
14. **Holt, S. C., and E. R. Leadbetter.** 1969. Comparative ultrastructure of selected aerobic spore-forming bacteria: a freeze-etching study. Bacteriol. Rev. **33**:346–378.
15. **Holt, S. C., and A. G. Marr.** 1965. Location of chlorophyll in *Rhodospirillum rubrum*. J. Bacteriol. **89**:1402–1412.
16. **Houwink, A. L.** 1953. A macromolecular monolayer in the cell wall of *Spirillum* spec. Biochim. Biophys. Acta **10**:360–366.
17. **Hylemon, P. B., J. S. Wells, Jr., N. R. Krieg, and H. W. Jannasch.** 1973. The genus *Spirillum*: a taxonomic study. Int. J. Syst. Bacteriol. **23**:340–380.
18. **Isaac, L., and G. C. Ware.** 1974. The flexibility of bacterial cell walls. J. Appl. Bacteriol. **37**:335–339.
19. **Kellenberger, E., A. Ryter, and J. Sechaud.** 1958. Electron microscope study of DNA-containing plasms. II. Vegetative and mature phage DNA as compared with normal bacterial nucleoids in different physiological states. J. Biophys. Biochem. Cytol. **4**:671–687.
20. **Kreig, N. R.** 1976. Biology of the chemoheterotrophic spirilla. Bacteriol. Rev. **40**:55–115.
21. **Liefson, E.** 1960. Atlas of bacterial flagellation. Academic Press Inc., New York.
22. **Martin, H. H., H. D. Heilmann, and H. J. Preusser.** 1972. State of the rigid layer in cell walls of some gram-negative bacteria. Arch. Mikrobiol. **83**:332–346.
23. **Moench, T. T., and W. A. Konetzka.** 1978. A novel method for the isolation and study of a magnetotactic bacterium. Arch. Microbiol. **119**:203–212.
24. **Murray, R. G. E.** 1963. On the cell wall structure of *Spirillum serpens*. Can. J. Microbiol. **9**:381–392.
25. **Murray, R. G. E., and A. Birch-Andersen.** 1963. Specialized structure in the region of the flagella tuft in *Spirillum serpens*. Can. J. Microbiol. **9**:393–401.
26. **Murray, R. G. E., P. Steed, and H. E. Elson.** 1965. The location of the mucopeptide in sections of the cell wall of *Escherichia coli* and other gram-negative bacteria. Can. J. Microbiol. **11**:547–560.
27. **Oppenheim, J., and L. Marcus.** 1970. Correlation of ultrastructure in *Azotobacter vinelandii* with nitrogen source for growth. J. Bacteriol. **101**:286–291.
28. **Remsen, C. C., S. W. Watson, J. B. Waterbury, and H. G. Truper.** 1968. Fine structure of *Ectothiorhodospira mobilis* Pelsh. J. Bacteriol. **95**:2374–2392.
29. **Reynolds, E. S.** 1963. The use of lead citrate at high pH as an electron-opaque stain in electron mciroscopy. J. Cell Biol. **17**:208–212.
30. **Ritchie, A. E., R. F. Keeler, and J. H. Bryner.** 1966. Anatomical features of *Vibrio fetus*: an electron microscope survey. J. Gen. Microbiol. **43**:427–438.
31. **Shively, J. M.** 1974. Inclusion bodies of prokaryotes. Annu. Rev. Microbiol. **28**:167–187.
32. **Sleytr, U. B.** 1978. Regular arrays of macromolecules on bacterial cell walls: structure, chemistry, assembly, and function. Int. Rev. Cytol. **53**:1–64.
33. **Spurr, A. R.** 1969. A low-viscosity epoxy resin embedding medium for electron microscopy. J. Ultrastruct. Res. **26**:31–43.
34. **Terasaki, Y.** 1972. Studies on the genus *Spirillum* Ehrenberg. I. Morphological, physiological, and biochemical characteristics of water spirilla. Bull. Suzugamine Women's Coll. Nat. Sci. **16**:1–146.
35. **Terasaki, Y.** 1973. Studies on the genus *Spirillum* Ehrenberg. II. Comments on type and reference strains of *Spirillum* and description of new species and new subspecies. Bull. Suzugamine Women's Coll. Nat. Sci. **17**: 1–71.
36. **Thorne, K. J. I.** 1977. Regularly arranged protein on the surfaces of Gram-negative bacteria. Biol. Rev. **52**:219–234.
37. **Williams, M. A., and S. C. Rittenberg.** 1956. Microcyst formation and germination in *Spirillum lunatum*. J. Gen. Microbiol. **15**:205–209.
38. **Wolin, E. A., M. J. Wolin, and R. S. Wolfe.** 1963. Formation of methane by bacterial extracts. J. Biol. Chem. **238**:2882–2886.